



HAL
open science

Tandem mass spectrometry enhances the performances of pyrolysis-gas chromatography-mass spectrometry for microplastic quantification

Magali Albignac, Tiago de Oliveira, Louisa Landebrit, Sébastien Miquel, Benoit Auguin, Eric Leroy, Emmanuelle Maria, Anne Françoise Mingotaud, Alexandra ter Halle

► To cite this version:

Magali Albignac, Tiago de Oliveira, Louisa Landebrit, Sébastien Miquel, Benoit Auguin, et al.. Tandem mass spectrometry enhances the performances of pyrolysis-gas chromatography-mass spectrometry for microplastic quantification. *Journal of Analytical and Applied Pyrolysis*, 2023, 172, pp.105993. <10.1016/j.jaap.2023.105993>. <hal-04097660>

HAL Id: hal-04097660

<https://hal.science/hal-04097660v1>

Submitted on 12 Oct 2023

HAL is a multi-disciplinary open access archive for the deposit and dissemination of scientific research documents, whether they are published or not. The documents may come from teaching and research institutions in France or abroad, or from public or private research centers.

L'archive ouverte pluridisciplinaire HAL, est destinée au dépôt et à la diffusion de documents scientifiques de niveau recherche, publiés ou non, émanant des établissements d'enseignement et de recherche français ou étrangers, des laboratoires publics ou privés.



HAL Authorization

1 Tandem mass spectrometry enhances the
2 performances of pyrolysis-gas chromatography-mass
3 spectrometry for microplastic quantification

4

5

6 *AUTHOR NAMES: Magali Albignac¹, Tiago de Oliveira¹, Louisa Landebrit¹, Sébastien Miquel²,*
7 *Benoit Auguin³, Eric Leroy⁴, Emmanuelle Maria¹, Anne Françoise Mingotaud¹, Alexandra ter*
8 *Halle^{1*}*

9 ¹ CNRS, Université Toulouse III, Laboratoire des Interactions Moléculaires et Réactivité Chimique et
10 Photochimique (IMRCP), UMR 5623, Toulouse, France

11 ² Thermo Fisher, Courtaboeuf, France

12 ³ Quad Service, Achères, France

13 ⁴ CNRS, Université Toulouse III, Institut de Chimie de Toulouse (ICT), UAR 2599, Toulouse, France

14

15 **KEYWORDS.** Plastic, polymer, nanoplastic, py-gc-ms, plastic debris

16

17 **ABSTRACT.** The ability of pyrolysis gas chromatography–mass spectrometry to quantify
18 microplastics has been demonstrated; this study aims to provide a robust method using tandem
19 mass spectrometry in order to gain in sensitivity and selectivity. The preparation of homogeneous
20 and repeatable solid standards allowed us to perform an external calibration for six polymers in

21 the nanogram range. Relevant indicator compounds were selected for each targeted polymer, and
22 multiple reaction monitoring optimization was undertaken. The linearity, standard deviation and
23 overall sensitivity were examined. After optimization, the detection limit was 15-70 ng according
24 to the polymer. Interferences between polymers were examined, and we demonstrated that tandem
25 mass spectrometry was necessary for the unequivocal detection of some polymers such as
26 polyethylene and polypropylene. The method was applied to analyze the plastic particle content in
27 bottled water. Only polyethylene terephthalate chemical compound was quantified at 42 ng.L⁻¹.
28 For future development, the use of internal standards will increase the method precision. It will
29 also be important to better understand the interferences with the matrix in complex samples and
30 the potential impact of weathering on the polymer pyrolytic response.

31 1. Introduction

32 Recent studies have shown that the natural environment¹, our food² and beverages³ are
33 contaminated with small plastic particles. Masses of plastic debris accumulate in the environment
34 due to a combination of high production, poor development of waste collection infrastructures and
35 low recycling volumes^{4, 5}. Environmental factors such as sunlight or mechanical stress promote
36 plastic debris fragmentation and erosion into very small particles⁶. The fate and route of
37 transportation of microplastics are poorly understood in relations to the risks associated with
38 ecosystem exposure or human health. This lack of awareness is mainly related to the need to
39 achieve fast and reliable methods to analyze microplastics in complex samples.

40 Several challenges arise with respect to the analysis of microplastics in environmental matrices.
41 Polymers in the samples have usually undergone weathering and profound structural
42 modifications, which makes sample preparation and identification challenging^{7,8}. The task is even
43 more challenging with smaller microplastics sizes to finally reach a knowledge and technology

44 gap below 150 μm ⁹. Very important analytical progress was achieved with spectroscopic
45 measurements. Breakthrough methods have emerged, e.g., with the development of automated
46 particle identification and data processing, which greatly reduced the time analysis and conferred
47 robustness to the methods^{10,11}. In parallel, pyrolysis–gas chromatography–mass spectrometry (Py-
48 GC–MS) appears to be a novel promising technique¹²⁻¹⁴. One of its interesting aspects is that it
49 does not have size limitations, which offers the possibility to analyze nanoplastics^{15,16}. The other
50 interesting potential in using Py-GC–MS is to overcome extensive sample preparation processes^{2,}
51 ^{17, 18}. Beyond detection, quantification was also performed ^{2, 18-22}. Quantification consists of
52 selecting one molecule among many decomposition products after pyrolysis to proceed to the
53 quantification; this specific molecule is called the indicator compound. Most described methods
54 monitor the indicator compounds using a simple quadrupole by ion extraction after full scan
55 recording^{19,23} or by single ion monitoring (SIM)^{2, 18, 20, 21}. The potentiality of mass spectrometry
56 was scarcely explored even if the gain from using high-resolution mass spectrometry was recently
57 proposed and the advantages were noticeable^{17, 24}. The aim of the study is to use tandem mass
58 spectrometry (Py-GC–MS/MS) in order to improve the sensitivity and selectivity of the analysis
59 with the achievement of lower limits of quantification. Since very low detection limits were
60 reached, we paid close attention to quality assurance and quality control to minimize
61 contamination during sample preparation and handling. For completion, the method was applied
62 to detect and quantify microplastics in bottled water.

63 2. Materials and Methods

64 2.1. Chemicals.

65 The polymers selected as external standards are high-density polyethylene (PE), poly(methyl
66 methacrylate) (PMMA), polyethylene terephthalate (PET), polycarbonate (PC), polystyrene (PS),

67 and polypropylene (PP), and their characteristics are listed in Table SI1. The selected indicator
68 compound standards are methylmethacrylate (MeMeta), 1,13 tetradecadiene (C14D), 1,9
69 decadiène (C10D), dimethylterphtalate (DMeTPh), 2,2-bis(4'-methoxy-phenyl)propane (BPAMe)
70 2,4-dimethylhept-1-ene (DMC7) 2,4,6-Triphenyl-1-hexene (SSS) and 2,4-diphenyl-1-butene (SS),
71 as listed in Table SI2. Tetramethylammonium hydroxide pentahydrate (TMAH) was purchased
72 from Sigma–Aldrich with a minimum purity of 97%. For the GC-MS/MS optimization, the
73 indicator compounds were dissolved in dichloromethane (VWR, Pennsylvania, USA). Absolute
74 ethanol (VWR, Pennsylvania, USA) was used to clean the materials. Ultra-pure water (18.2 MΩ
75 cm) was obtained from a Milli-Q filtration unit (Merck Millipore, MA, USA).

76

77 2.2. Quality Assurance and Quality Control (QA and QC).

78 Koealmans et al. recently stressed the need for stricter QA when analyzing microplastics in water
79 samples³. Their recommendations were considered, and special care was taken to minimize
80 contamination. Cotton lab clothes were adopted to avoid any risk of contamination from synthetic
81 materials. The use of cotton masks was preferred to synthetic masks, since the experiments were
82 conducted during covid19 pandemic. Sample handling was performed in a clean air laboratory
83 under a daily cleaned hood. Sample preparation was only performed with glass or metal
84 equipment. All glassware was pretreated by calcination at 550 °C: 1.5 h of heating from room
85 temperature to 550 °C, 1.5 h of holding at this temperature and slow cooling overnight using an
86 LV 5/11 furnace from Nabertherm®. The glass fiber filters (GF/F, porosity 0.7 μm, Whatman®)
87 were prepared after an optimized calcination to remove any trace polymer and consisted of heating
88 from room temperature to 500 °C at a rate of 80 °C/hour with a hold of 30 hours at 500 °C in the
89 same furnace. The furnace programming optimization was realized by analyzing the filter by Py-

90 GC-MS/MS; especially the remaining signal of PE was monitored as it was relatively initially
91 important in the filters. The cells for cryogenic grinding (SPEX® SamplePrep 6775 Freezer/Mill
92 cryogenic Grinder, Delta Labo, France) were always cleaned before any use: first by calcination
93 and subsequently by washing with ethanol and kintex tissue (high-performance wiper 7624 from
94 Kimberly-Clark Professional®). The use of an appropriate methylation agent was optimized
95 regarding contamination introduction. The pyrolysis quartz tubes (from Quad Service, France)
96 were freshly pre-calcined at 1000 °C. The quartz tubes were weighed before and after adding
97 samples using a Micro Balance from Sartorius (MCE225P-2S00-A Cubis®-II Semi) with a
98 sensitivity of 0.01 mg. The samples were placed in an inox sample holder under a glass bell to dry
99 for 1 hour before being placed into the pyrolysis autosampler.

100

101 2.3. Preparation of external calibration standard.

102 All polymers were first cryo-milled using the SPEX® cryogenic Grinder. The cryo-milling
103 program was as follows: precool 2 min; run 1 min; cool 2 min; cycles 15; cps 15. Then, the ground
104 polymers were mixed with an inert glass fiber matrix. This inert matrix was prepared from glass
105 fiber filters that were cryo-milled (precooled for 1 min; cooled for 1 min; cycled 6; cps 15) and
106 calcined. The standards were first prepared at concentrations of 1-5 mg.g⁻¹ depending on the
107 polymer (Table SI3). The powder was first diluted by a factor of 10 (powder 2, table SI3), and 5
108 following external standards were obtained by further dilution (Table SI3). The standards were
109 weighed in quartz tubes using a Micro Balance.

110

111

112

113 2.4. Py-GC-MS/MS analysis.

114 Pyrolysis experiments were performed in a CDS Analytical Pyroprobe® Model 6150 (QUAD
115 SERVICE, Achères, France) interfaced with a GC-MS/MS triple quadrupole TSQ® 9000 from
116 Thermo Fisher Scientific (Villebon sur Yvette, France). The gas chromatography column was a
117 TraceGOLD TG-5SilMS from Thermo Fisher Scientific. The optimized experimental parameters
118 for Py-GC-MS/MS are summarized in Table SI4. Multiple reaction monitoring (MRM)
119 optimizations for collision energy were obtained using Auto SRM 4.0 from Chromeleon®. MRM
120 optimization was performed with the pure indicator compounds in liquid injection with a Thermo
121 Scientific® AI/AS 1310 autosampler. There was an exception for the PP second indicator
122 compound, for which the diastereoisomers of the 2,4,6,8-tetramethyl-1-undeceneseries (TeMC11)
123 were not easily commercially available; thus, the optimization was performed from the pyrolysis
124 of PP. The MS acquisition parameters are listed in Tables SI5 and SI6. The
125 confirmation/quantification ratios were first established based on the chromatographic peaks after
126 liquid injection and compared to those in the pyrolysis injection mode (Table SI5 and SI6).
127 Chromatographic peaks were integrated using the Cobra detection algorithm from the
128 Chromeleon® 7.2.8 software. For the pyrolysis, approximately 2 mg of external standards or
129 sample was weighed in a quartz tube (ref 6201-3004, QUAD SERVICE, Achères, France) on a
130 Sartorius Micro Balance. Then, online derivatization was performed with 5 µL of aqueous TMAH
131 solution (25 wt %), which was directly spiked inside the pyrolysis tubes using a microsyringe
132 (VWR, Pennsylvania, USA). The limits of detection and quantification (LOD and LOQ
133 respectively) were defined with the classical criteria:

$$134 \quad LOD = \overline{blank} + 3 \times (\textit{standard deviation Procedural blank})$$

$$135 \quad LOQ = \overline{blank} + 10 \times (\textit{standard deviation Procedrual blank})$$

136 A compound was determined if the specific retention time deviation was less than 0.1 min and
137 the ratio Tc/Tq deviation was less than $\pm 30\%$ compared to the standards.

138

139 2.5 Sample preparation.

140 Several bottles of mineral water purchased from the closest supermarket (Brand Eco +® 1.5 L
141 from E.Leclerc) were filtered to obtain a total filtered volume of 20 L. The bottles made in PET
142 were made of pristine polymer but it was indicated that the bottles were reusable, they were with
143 a cap in PP. Filtrations were achieved using a Masterflex® IP33 Digital LED Variable-Speed
144 Pump Drive from Cole-Parmer France, associated with a Masterflex® silicone tubing (Platinum)
145 L/S®²⁴ (Cole-Parmer France) and an inox 1209 In-Line filter holder 25 mm from Pall Corporation
146 (State of New York, USA). The tubing and filter holder unit limited the air exchanges and avoided
147 any atmospheric deposition onto the glass fiber filter. Water filtration was performed on pre-
148 calcined and weighed glass microfiber filters. For negative control we used MilliQ water that was
149 filter on calcined glass fiber filters in closed calcined glass unit. This water was stored in calcined
150 glass bottles. The negative controls consisted of filtering this prepared with the exact same protocol
151 used for the sample. After the water filtration, the filters from the sample and negative control
152 were dried at 30 °C for 24 h in a closed glass petri dish, weighed and cryo-ground. Possible milling
153 contamination was evaluated by grinding a calcined filter. In total, 6 replicates of cryo-ground
154 filters, sample and negative control were analyzed. To consider the Py-GC/MS-MS signal intensity
155 deviation, all external calibration standards and samples were analyzed in the same sequence on
156 the same day.

157

158 3.Results and discussion

159 The method was developed for the most commonly used polymers: PMMA, PP, PE, PET, PS and
160 PC. This is a common selection among the published Py-GC-MS developments¹². The present
161 study is not dedicated to investigating the matrix effect or polymer weathering impact on the
162 pyrolytic response; these important aspects will be discussed in future work. The method
163 development was conducted with an external calibration and applied to measure the polymer
164 content in bottled water, where there should be no matrix interferences, and the present polymer
165 certainly resulted from the manufacturing processes not weathered.

166 3.1. Indicator compound selection

167 The selection of indicator compounds for quantification was recently argued in a critical review,
168 and it is consensual for most polymers (Table SI5)¹². In addition to the detection of one indicator
169 compound (I_1), it was recently proposed to select a second one (I_2) when it is possible to record
170 their ratios (I_2/I_1) as additional validation criteria². For PE, PP and PS, as several decomposition
171 products were formed in important proportions, a second indicator compound was recorded, and
172 the ratio (I_2/I_1) was used as an additional validation criterion (Table SI 6).

173 For PE, many options remain open in terms of indicator compound selection¹². The PE pyrolysis
174 yields several hundred different hydrocarbons: linear or branched and containing 0 to 2 C-C double
175 bound. The large number of peaks with relatively equal intensity suggests that the pyrolysis
176 mechanism started with random scission. The pyrograms show a suite of equally spaced
177 multiplets²⁵, which are often referred to as triplets considering the three most intense peaks. The
178 triplet is successively composed of a terminal n-alkadiene (also called α,ω -alkadienes, C_nD)
179 followed by a terminal n-alkene (C_nE) and an n-alkane (C_nA). The second peak shows the highest

180 response. CnE and CnA are not specific to the PE pyrolysis because natural organic matter
181 pyrolysis produces these molecules, whereas CnD was identified to be more specific to PE
182 pyrolysis²⁶. CnD was formed in a much lower amount than the mono- or unsaturated congeners,
183 and for the detection limit constraints, it was often proposed to monitor the mono unsaturated
184 congeners but in counterpart with an intensive sample purification to avoid matrix interferences²⁰,
185 ^{21, 27}. The higher sensitivity of the MS/MS detection allowed us to select the indicator compounds
186 among the α,ω -alkadienes; congeners with 14 and 15 carbon atoms (C14D and C15D) were
187 selected because they were the most intense and well-resolved peaks (Table SI5 and SI6). The PP
188 pyrolysis generates branched-chain hydrocarbons with a predominantly unsaturated structure. The
189 selected indicator compounds are the two most intense peaks: 2,4-dimethylhept-1-ene (DMC7)
190 and the most abundant diastereoisomer among the 2,4,6,8-tetramethyl-1-undecene series
191 (TeMC11).

192

193 3.2. Instrument method development and MS/MS optimization

194 Working with pyrolysis, typically 1-2 mg of sample is weighed and introduced into the pyrolysis
195 chamber. The repeated introduction of a solid sample is susceptible to larger experimental
196 uncertainties than an automated liquid injection in the GC/MS system. Nonetheless, analytical
197 pyrolysis later instrumental developments allowed us to provide a stable signal with a relative
198 standard deviation (RSD) of 10-15% without internal standard corrections ^{28, 29}, and good
199 correlation values were presented for the calibration curves^{2, 28}. Using a simple quadrupole and
200 working with traditional polymers, Fischer et al.^{20, 21}, for example, provided external calibration
201 between 0.4 and 1070 μg . The lowest point of the calibration was a consequence of the limit of the

202 precision of the scale and the author explained that at this concentration the signal to noise ratio
203 was important. Ribeiro et al.² or Okoffo et al.¹⁸ analyzing microplastic in seafood tissues or in
204 biosolid respectively, worked with calibration curves linear in the range 0.02 to 10 μg . These two
205 studies presented low limit of quantification after sample extraction containing a step of
206 pressurized liquid extraction from 0.07 to 24.3 $\mu\text{g}\cdot\text{g}^{-1}$ tissue² or from 0.03 to 0.37 $\mu\text{g}\cdot\text{g}^{-1}$ ¹⁸. External
207 standards in this range were carefully prepared by solid dilution in an inert matrix to provide good
208 homogeneity (Table SI3). It was recently discussed that the solid diluent could act as a catalyst in
209 the pyrolysis of some polymers, favoring the formation of different pyrolytic indicator compounds
210 and thus impacting the quantification³⁰. The authors showed that deactivated silica was very
211 promising solid³⁰. Here we have opted to used cryo-milled glass fiber filters because during sample
212 preparation the sample (here bottled water) was filtered on glass fiber to collect and transfer the
213 plastic particles to the pyrolysis chamber. The external calibration is then prepared in the exact
214 same solid matrix as the sample. Briefly, we added a given amount of the initial powder to cryo-
215 milled and calcined glass fiber filters. The mixture was again homogenized by cryo-milling
216 because simple shaking was not sufficient enough. The homogeneity of the powder was controlled
217 by repeated injection in Py-GC-MS/MS. We particularly recommend strictly restricting the
218 amount of introduced polymer to the nanogram range to prevent source fouling or possible
219 deterioration of the analyzer. Often, sample preparation consists in digestion and/or density
220 separation; the last step of the sample preparation can be a filtration. The filter is first, a mean to
221 collect and transfer the particles to the pyrolysis chamber but also a dilution media. Dilution factor
222 that can be adjusted by the diameter and thickness of the glass fiber filter. After the homogenization
223 steps have been optimized, the measured RSD over 6 replicates was 6-25% in the concentration
224 range of 90-460 $\mu\text{g}\cdot\text{g}^{-1}$, depending on the polymer.

225 The source transfer line and injector temperatures were optimized (Table SI4). The pyrolysis
226 temperature was optimized by Hermabessierre et al. for PE, PC and PET³¹. We examined the
227 pyrolysis temperature effect for the six selected polymers at 550-750 °C with standard calibration
228 powder number 2 (table SI3). The PE response was the faintest due to the selection of CnD as an
229 indicator compound, which was considered when selecting the optimized pyrolysis temperature of
230 600 °C (Figure SI1).

231 Since polymer pyrolysis generates a large number of molecules, pyrograms are very complex. We
232 ensured that the detection and attribution of every indicator compound was free of interferences.
233 To do so, the MS/MS detection parameters were optimized in liquid injection using the pure
234 molecules as standards (Table SI2). The MRM responses were compared to those obtained after
235 pyrolysis with the polymers alone or in mixture. After the GC condition optimization, we ensured
236 that for all indicator compounds considered, there was less than 10% variation in the ion transition
237 confirmation to quantification ratios (T_c/T_q) between GC-MS/MS and Py-GC-MS/MS (Table
238 SI5). The particular case of PP is discussed in detail in the next section.

239 For PMMA, PET and PC detection, the use of TMAH as a methyl agent was necessary. According
240 to Fischer et al., the use of TMAH does not affect the detection of other polymers²¹; this was
241 verified under the present analytical conditions. To reduce the noise of the measure, we
242 recommend the use of TMAH in crystals and the preparation of a solution at 25 wt % in ultra-pure
243 water that was filtered on 0.1- μ m PTFE Omnipore® membranes (47-mm diameter, Sigma-
244 Aldrich) instead of using a commercial solution. In the full scan, we observe that DMC7
245 systematically co-eluted with a substance, which we attributed to be a product of the
246 decomposition of TMAH (mass spectra of the substance in Figure SI2). Full separation was not
247 achieved regardless of the tested GC conditions (temperature program, length of the column; data

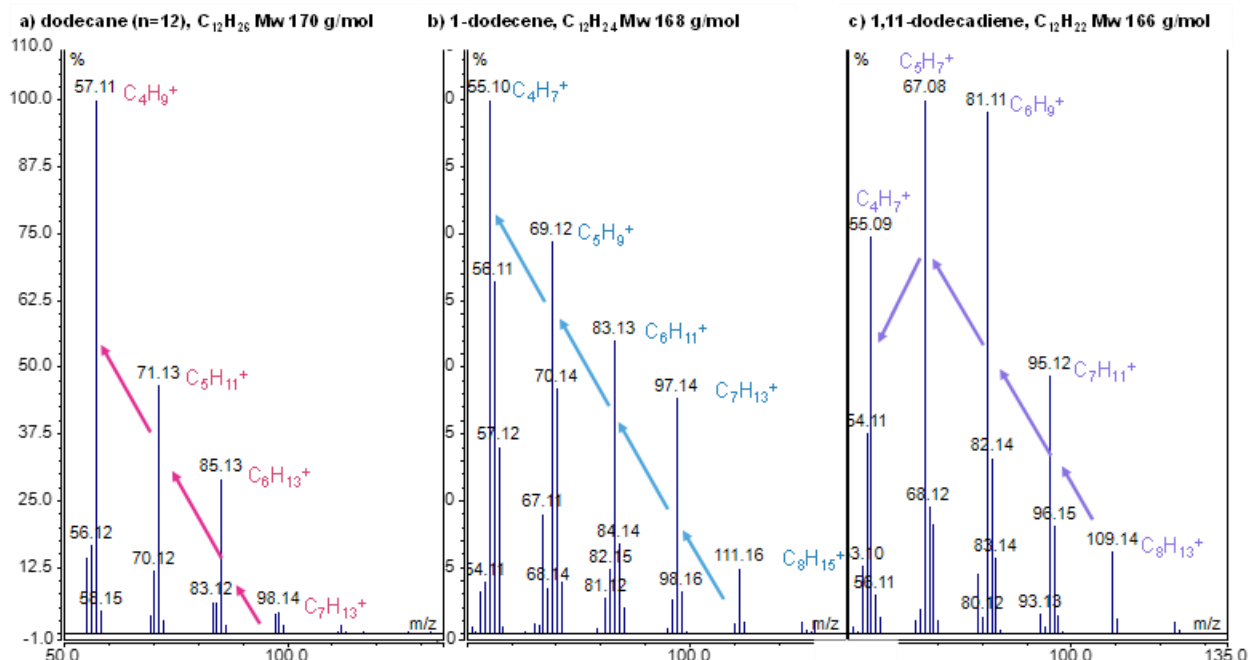
248 not shown). In MRM, DMC7 is not altered with the optimized transition, but we recommend
249 caution in the SIM mode. DMC7 monitoring (ions at m/z 70 and 126) shows an alteration of the
250 ratio if PP was analyzed pure diluted in glass fiber filter (ratio 12%) or in the standard mixture
251 with TMAH (ratio 20%, data not shown).

252 3.3. Particular case of the hydrocarbon mass spectra

253 PE and PP are the most frequently detected polymers in the environment. They decompose into
254 hydrocarbons that are not easily detected in mass spectrometry, so it is important to detail their
255 responses. Straight-chain alkane molecular ions are usually weak. The molecular ions of the
256 unsaturated derivatives are slightly more intense. It can be interesting to investigate lower collision
257 energy, for example 30 eV, in order to enhance the signal of the hydrocarbon molecular ions. In
258 the present study, the bottled waters tested present a simple matrix and the gain in selectivity
259 working at lower collision energy and monitoring higher m/z ions was not significant (data not
260 shown). For alkanes, the base peak in the mass spectra is usually at m/z 57 and corresponds to the
261 C_4H_9 carbocation; it is surrounded by other smaller peaks due to the hydrogen atom rearrangement.
262 The groups are separated by 14 atomic mass units, which result from the loss of radical CH_2 (Figure
263 1). For alkanes, the larger peak in the multiplets corresponds to the molecular formula C_mH_{2m+1} .
264 With the same reasoning, the mass spectra of alkenes and α,ω -alkadienes contain carbocations at
265 C_mH_{2m-1} and C_mH_{2m-2} , respectively (Figure 1 b and c). The base peak corresponds to the
266 carbocation with $m=4$; the exponential decay of the longer carbocations indicates a linear
267 hydrocarbon. Prominent peaks with longer carbocations are typical for branched congeners (Figure
268 SI3 shows an example with alkene).

269

270

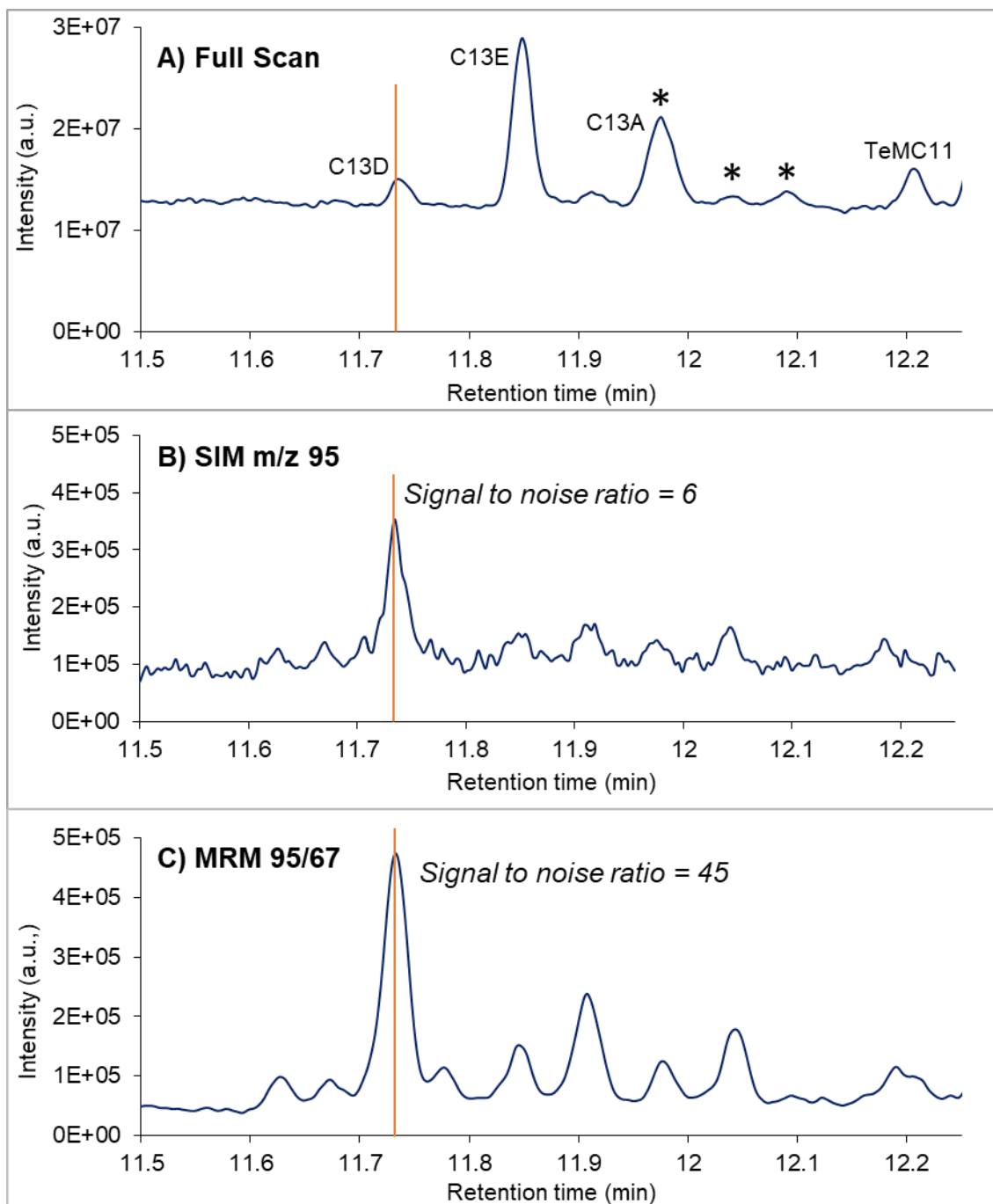


272

273 Figure 1: Mass spectra of a) alkane, b) alkene and c) α,ω -alkadiene with $n=12$. The arrow
 274 represents a loss of CH_2 . The formula in bold character on top of each cluster corresponds to the
 275 most intense peak. For alkanes, the base peak is at m/z 57 and corresponds to the C_4H_9 carbocation;
 276 for n -alkenes, it is at m/z 55 and corresponds to C_4H_7 ; for α,ω -alkadienes, the base peak is at m/z
 277 67 (the C_5H_7), but the ion m/z 55 is also intense. The 3 hydrocarbons present distinct degrees of
 278 unsaturation but nonetheless have many ions in common.

279 To summarize, among hydrocarbons, both structural isomers and congeners with distinct levels of
 280 unsaturation have common ions (Figure 1). In addition, the use of high-resolution GC revealed the
 281 complexity of the mixture of a pyrolyzate. For example, in the case of PE, more than 140 different
 282 molecules were identified for congeners with 8 carbon atoms. Evidently, the use of classical GC
 283 does not fully separate the isomers²⁵.

284 Figure 2 illustrates the response of the standard mixture magnified in the region of PE congeners
285 with 13 carbon atoms in full scan, single ion monitoring and multiple reaction monitoring mode.
286 The pyrogram is complex and PE indicator compound (the alkadiene) was surrounded by many
287 peaks. The mass spectra of the peaks obtained from the full scan show co-eluting substances (Table
288 SI7). We observed here that the peak ratios in SIM or MRM mode for the pure polymer or in the
289 standard mixture were not modified (Table SI7). In the premises of microplastic analysis by Py-
290 GC-MS the use of ratios was not systematically adopted to validate the detection of the peaks^{20,21,}
291 ^{26,27}. In SIM mode, several ions were more recently monitored ^{2,18}. As it was already reported in
292 SIM mode, some ratios can be altered in a complex sample³² so we recommend to use these
293 criteria. As an additional validation step, we have analyzed the pure substances in liquid injection
294 and made sure the ratios were the same to the pyrograms. Finally, the signal to noise ratio in
295 MS/MS were superior to SIM experiment (Figure 2).



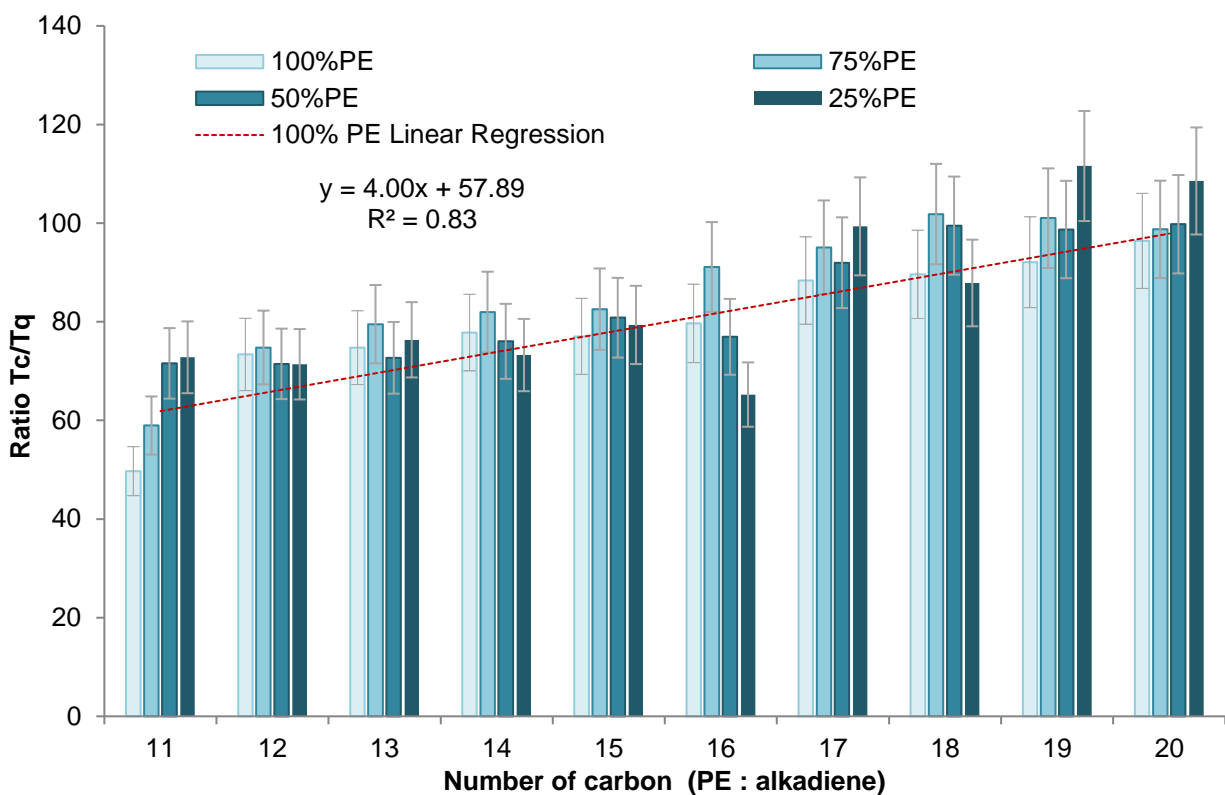
296

297 Figure 2: A) Total ion current in full scan (TIC) of a mixture of 6 pyrolyzed polymers. The triplet
 298 specific to PE pyrolysis (at 700 ng) is presented, which is composed of the three congeners α,ω -
 299 alkadiene, n-alkene and n-alkane (C13D marked with an orange line, C13E and C13A). The peak
 300 labeled TeMC11 resulted from the PP pyrolysis. The peaks marked with a star were identified as

301 the result of a mixture of co-eluting molecules after an examination of their mass spectra in the
302 full scan. B) Single ion monitoring and C) Multiple reaction monitoring.

303 3.4. PE and PP possible interferences

304 We recommend paying particular attention to the PE and PP interferences during method
305 development, since all degradation products are hydrocarbons, and some indicator compounds
306 present relatively similar Kovats retention indices. This was investigated with PE and PP mixtures
307 in an inert matrix in proportions of PE/PP: 3/1; 1/1: and 1/3. The ratio T_c/T_q for C_nD was recorded
308 (Figure 3). Interestingly, there was a linear correlation between T_c/T_q and the diene length. With
309 $n=16$, the introduction of increasing amounts of PP showed an anomaly. Some PP decomposition
310 products were co-eluting with this congener under the chromatographic conditions. Similar
311 interactions were recorded with C_nA and C_nE (Figure SI4). During method development, it is
312 recommended to ensure that such interferences do not occur with the selected indicator
313 compounds.



314

315 Figure 3: Recording of the ion transitions Tc/Tq (m/z 109>67 and 95>67) when pyrolyzing a
 316 mixture of PE and PP with PE/PP ratios of 3/1, 1/1: and 1/3. for CnD.

317 As previously mentioned, the MRM response of the indicator compounds was recorded with pure
 318 standards in liquid injection with the exception of TeMC11, which was not easily commercially
 319 available. Thus, it was important to pay particular attention to this peak and verify that there was
 320 no coelution. The peak was identified using its Kovats retention index (data from PubChem® for
 321 a standard nonpolar column), and its attribution was confirmed by comparing the mass spectra of
 322 the peak to the literature^{33, 34}. We ensured that the mass spectra of this peak and the relative
 323 proportion of the major ions did not change when PP was pyrolyzed alone or in mixture with other
 324 polymers.

325 The ratio I₂/I₁ was determined for PS, PE and PP. For PE, the ratio was remarkably stable over the
 326 entire study, injected alone or in mixture with other polymers (RSD 8%). For PP, the ratio was

327 also stable (RSD 12%). In addition to the selected polymer to produce the external standards, other
328 PP references were tested, and the ratio was consistent (homo or copolymers). In SIM mode, the
329 monitoring DMC7 (m/z 70 and 126) and TeMC11 (m/z 111 and 83), the ratios were not altered by
330 the presence of PE. For PS, there was more variation in the ratio (28%); this result was not
331 rationalized.

332

333 3.5. External standard calibration and limit of quantification.

334 The method was conducted with external calibration. The use of internal standard calibration was
335 described for PS. This isotopic analog is commercially available; since PS is soluble in common
336 solvent at room temperature, spiking is easy to repeat^{28,35}. Since the isotopic analogs for the other
337 polymers were not commercially available, we opted for external calibration. The R² values were
338 0.92-0.98 depending on the selected polymer (Table SI7 and Figure SI5) and highlighted a
339 satisfactory correlation signal to the polymer amount.

340 The limits of MS/MS performances (analytical sensitivity) were not reached in this method
341 development because at the lowest calibration points, the signal-to-noise ratios exceeded 10 for all
342 considered indicator compounds. The analytical sensitivity was much lower than the LOQ and
343 LOD. The LOD and LOQ were higher because of cross-contamination even if we pay particular
344 attention to limiting it. There was a constant residual signal with the concentration point zero. The
345 LOQ and LOD were in the range of nanograms per liter (as listed in Table S1).

346 **Table 1:** Listing of calibration data for the investigated polymer and analytical limit. As a
347 comparison to Py-GC-MS performances, analytical limits with an [external calibration were](#)
348 [reported](#)²⁰. In this study, it was specified that the limit of the method was the precision of the
349 [balance](#). Similarly, limits were later reported down to 500 ng and with the use of dissolved PS
350 [the LOD reached 30 ng for this polymer](#)²¹. Finally in studies dedicated to the monitoring

351 microplastic content in seafood the calibration curves were linear in the range 0.02 to 10 µg and
 352 the LOQ were from 0.07 to 24.3 µg.g⁻¹ tissue². In biosolids the LOQ were between 0.03 to 0.37
 353 µg.g⁻¹¹⁸.

Polymer	(I1)	N	Calibration functions	R ²	Analytical limit (ng)	Reported limit of quantifications
PMMA	MeMeta	16	y = 3190.7x - 50154	0.9398	20	< 0.4 µg
PP	DMC7	15	y = 2702.8x + 9264.9	0.9470	20	< 0.6µg
PE	C14D	16	y = 16.669x - 122.49	0.9873	70	< 50 µg
PET	DMeTPh	14	y = 11968x - 148766	0.9307	15	< 5µg
PC	BPAMe	16	y = 112187x - 344480	0.9248	15	> 2.7 µg
PS	SSS	14	y = 3671.1x - 74477	0.9587	30	> 1.5 µg

354

355

356 3.5. Application to the bottled water analysis.

357 To apply this newly developed method, the polymer content in bottled water was determined. We
 358 selected this simply sample because it was reasonable to assume that there would be no matrix
 359 interferences, the present microplastics would certainly come from the manufacturing processes,
 360 and they consequently did not undergo weathering. We did not investigate these two aspects, but
 361 matrix interference^{14,36} and polymer weathering^{37,38} were reported to impact the polymer pyrolytic
 362 response.

363 After filtering 20 L of bottled water through a GF/F glass fiber filter, cryo-grinding and analyzing
364 the sample using Py-GC-MS/MS, we only determined the PET content. The other polymer
365 concentrations were below the LOD (details of the LOQ levels are shown in Table SI8). The PET
366 concentration in mineral water was measured at $42 \pm 20 \text{ ng.L}^{-1}$. The concentration presented after
367 6 consequent analyses of the sample presented an important standard deviation of 50%. Two values
368 were particularly high compared to the others, if we remove these values the standard deviation
369 drops to 13% (n=4), the concentration was thus determined at 28 ng/L (Table SI 9). The outliers
370 are certainly the result of air contamination while the sample remained on the autosampler module
371 (a couples of hours).

372 The microplastic content in bottled water has been mainly determined using micro-Fourier
373 transform infrared spectroscopy (μ -FTIR)^{3, 39} or micro-Raman spectroscopy^{40, 41}. Both techniques
374 exhibited particle size limitations and did not provide the mass concentrations. For example,
375 Ossmann et al.⁴⁰ found an average concentration of 2649 (RSD \pm 2857) particles.L⁻¹ with 53.6%
376 of the particles under a size of 1.5 μm and 44.7% in the range of 1.5-5.0 μm ⁴⁰. Polymer type ratio
377 showed that 78% of the detected microplastics were PET, and the remainder was defined as olefins.
378 We converted these results to mass concentration by assuming that the particles were spherical
379 with a mean radius of 1.5 μm and using the known density of the specific polymer. We found a
380 theoretical mass concentration of 2.62 ng.L⁻¹ for PET and 0.23 ng.L⁻¹ for olefins. With a radius of
381 5 μm , the PET concentration was 30 times higher (Table SI10). This result illustrates that the
382 particle size is the major parameter that drives the variation in mass concentration. The determined
383 PET concentration here was within the range given by Obmann et al. (0-81 ng.L⁻¹)⁴⁰.
384 Since Py-GC-MS/MS does not provide any information about particle size or number of particles,
385 the obtained data here were converted the other way: 28 ng/L is estimated to correspond to 12000

386 and 320 particles.L⁻¹ using mean particles diamaters of 1.5 μm and 5 μm respectively.. These kinds
387 of calculations need to be treated with lot of care and are recommendable for rough comparison
388 only. The conversion between mass and number of particles, and vice versa, allows us to concluded
389 that studies using spectroscopic measurements ⁴⁰ and the one presented here leads to the same
390 range of concentrations.

391

392 3.6. Use of MS/MS requirements.

393 Facing the tremendous complexity of a pyrogram, the accuracy of TOF-MS²⁴ or the selectivity of
394 MS/MS drastically improves the performance of Py-GC-MS¹⁷, as demonstrated here. These types
395 of mass spectrometers have not been extensively tested with pyrolysis, certainly because the cost
396 of purchase is limiting compared to simple quadrupole. The reason may be that a routine analysis
397 using a simple quadrupole is sufficiently complex. The use of high-performance spectrometers
398 requires highly specialized personnel and an important time implication for their maintenance.
399 Pyrolysis is known to induce source fouling and column bleeding, so the signal quality must be
400 monitored. We very regularly maintained the instrument. For example, the PET indicator
401 compound peak broadening rapidly occurred and was solved with a maintenance of the GC
402 column. Nonetheless, the use of high-performance spectrometers offers many promising
403 perspectives, such as the development of high-throughput sample analysis, which is an important
404 step toward the achievement of risk assessment studies.

405

406 4. Conclusion

407 In conclusion, the first goal of this study was to demonstrate the important improvements provided
408 by using MS/MS. PP and PE were used to illustrate the unequivocal attribution of their indicator

409 compounds using MRM experiments. The second aspect is the gain in detection limits, which
410 reached the ng/L range, with MS/MS. Even if we took great care to control cross contamination,
411 there was still polymer traces in the procedural blank. The limit of the study was the control of the
412 cross contamination and not the performances of the mass spectrometer. Finally, the use of isotopic
413 analogs to develop the internal standards will drastically improve the precision of the measure but
414 is challenging³⁵. Some aspects should be investigated to provide a robust method in complex
415 samples. For matrix interferences, there is a balance between reducing the purification steps and
416 controlling the matrix interferences^{2, 18}. Weathering also impacts the pyrolytic response of
417 polymers, which must be addressed to provide a method to estimate the uncertainties of the
418 measure^{36, 38}.

419 ASSOCIATED CONTENT

420 **Supporting Information.** Supplementary data related to this article can be found at

421 AUTHOR INFORMATION

422 **Corresponding Author**

423 *Alexandra ter Halle: alexandra.ter-halle@cnrs.fr

424 **Author Contributions**

425 The manuscript was written with contributions of all authors. All authors have given approval to
426 the final version of the manuscript.

427 **Funding Sources**

428 This work was supported by the ANR (Agence Nationale de la Recherche) PRC program
429 through the PEPSEA project (ANR- 17-CE34-0008-05).

430 ACKNOWLEDGMENTS

431 We acknowledge Julien Gigault and Bruno Grassl for the vivid and passionate discussion about
432 polymer pyrolysis.

433 REFERENCES

434

- 435 1. Rochman, C., Microplastics research - from sink to source. *Science* **2018**, *360*, (6384),
436 28-29.
- 437 2. Ribeiro, F.; Okoffo, E. D.; O'Brien, J. W.; Fraissinet-Tachet, S.; O'Brien, S.; Gallen, M.;
438 Samanipour, S.; Kaserzon, S.; Mueller, J. F.; Galloway, T.; Thomas, K. V., Quantitative
439 Analysis of Selected Plastics in High-Commercial-Value Australian Seafood by Pyrolysis Gas
440 Chromatography Mass Spectrometry (vol 54, pg 9408, 2020). *Environ. Sci. Technol.* **2020**, *54*,
441 (20), 13364-13364.
- 442 3. Koelmans, A. A.; Hazimah Mohamed Nor, N.; Hermesen, E.; Kooi, M.; Mintenig, S. M.;
443 De France, J., Microplastics in freshwaters and drinking water: Critical review and assessment of
444 data quality. *Water Research* **2019**, 410-422.
- 445 4. Geyer, R.; Jambeck, J.; Lavender Law, K., Production, use, and fate of all plastics ever
446 made. *Science Advances* **2017**, (7).
- 447 5. Jambeck, J. R.; Geyer, R.; Wilcox, C.; Siegler, T. R.; Perryman, M.; Andrady, A.;
448 Narayan, R.; Law, K. L., Plastic waste inputs from land into the ocean. *Science* **2015**, *347*,
449 (6223), 768-771.
- 450 6. Thompson, R. C.; Olsen, Y.; Mitchell, R. P.; Davis, A.; Rowland, S. J.; John, A. W. G.;
451 McGonigle, D.; Russell, A. E., Lost at sea: Where is all the plastic? *Science* **2004**, *304*, (5672),
452 838-838.
- 453 7. ter Halle, A.; Ladirat, L.; Martignac, M.; Mingotaud, A. F.; Boyron, O.; Perez, E., To
454 what extent are microplastics from the open ocean weathered? *Environ. Pollut.* **2017**, *227*, 167-
455 174.
- 456 8. Rowenczyk, L.; Dazzi, A.; Deniset-Besseau, A.; Beltran, V.; Goudouneche, D.; Wong-
457 Wah-Chung, P.; Boyron, O.; George, M.; Fabre, P.; Roux, C.; Mingotaud, A. F.; ter Halle, A.,
458 Microstructure Characterization of Oceanic Polyethylene Debris. *Environ. Sci. Technol.* **2020**,
459 *54*, (7), 4102-4109.
- 460 9. Schwaferts, C.; Niessner, R.; Elsner, M.; Ivleva, N. P., Methods for the analysis of
461 submicrometer- and nanoplastic particles in the environment. *Trends Anal. Chem.* **2019**, *112*, 52-
462 65.
- 463 10. Primpke, S.; Lorenez, C.; Rascher-Friesenhausen, R.; Gerdts, G., An automated approach
464 for microplastics analysis using focal plane array (FPA) FTIR microscopy and image analysis.
465 *Anal Methods* **2017**, *9*, 1499.
- 466 11. Cowger, W.; Gray, A.; Christiansen, S. H.; DeFrono, H.; Deshpande, A. D.;
467 Hemabessiere, L.; Lee, E.; Mill, L.; Munno, K.; Ossmann, B. E.; Pittroff, M.; Rochman, C.;
468 Sarau, G.; Tarby, S.; Primpke, S., Critical Review of Processing and Classification Techniques
469 for Images and Spectra in Microplastic Research. *Applied Spectroscopy* **2020**, *74*, (9), 989-1010.
- 470 12. Yakovenko, N.; Carvalho, A.; ter Halle, A., Emerging use thermo-analytical method
471 coupled with mass spectrometry for the quantification of micro(nano)plastics in environmental
472 samples. *TrAC Trends in Analytical Chemistry* **2020**, *131*, 115979.

- 473 13. Fabbri, D.; Rombola, A. G.; Vassura, I.; Torri, C.; Franzellitti, S.; Capolupo, M.; Fabbri,
474 E., Off-line analytical pyrolysis GC/MS to study the accumulation of polystyrene microparticles
475 in exposed mussels. *Journal of Analytical and Applied Pyrolysis* **2020**, *149*.
- 476 14. Pico, Y.; Barcelo, D., Pyrolysis gas chromatography-mass spectrometry in environmental
477 analysis: Focus on organic matter and microplastics. *Trac-Trend Anal Chem* **2020**, *130*.
- 478 15. ter Halle, A.; Jeanneau, L.; Martignac, M.; Jarde, E.; Pedrono, B.; Brach, L.; Gigault, J.,
479 Nanoplastic in the North Atlantic Subtropical Gyre. *Environ. Sci. Technol.* **2017**, *51*, (23),
480 13689-13697.
- 481 16. Sullivan, G. L.; Gallardo, J. D.; Jones, E. W.; Holliman, P. J.; Watson, T. M.; Sarp, S.,
482 Detection of trace sub-micron (nano) plastics in water samples using pyrolysis-gas
483 chromatography time of flight mass spectrometry (PY-GCToF). *Chemosphere* **2020**, *249*.
- 484 17. Albignac, M.; Ghiglione, J. F.; Labrune, C.; ter Halle, A., Determination of the
485 microplastic content in Mediterranean benthic macrofauna by pyrolysis-gas chromatography-
486 tandem mass spectrometry. *Marine Pollution Bulletin* **2022**, *181*, 113882.
- 487 18. Okoffo, E. D.; Ribeiro, F.; O'Brien, J. W.; O'Brien, S.; Tscharke, B. J.; Gallen, M.;
488 Samanipour, S.; Mueller, J. F.; Thomas, K. V., Identification and quantification of selected
489 plastics in biosolids by pressurized liquid extraction combined with double-shot pyrolysis gas
490 chromatography-mass spectrometry. *Sci. Total Environ.* **2020**, *715*.
- 491 19. Eisentraut, P.; Dumichen, E.; Ruhl, A. S.; Jekel, M.; Albrecht, M.; Gehde, M.; Braun, U.,
492 Two Birds with One Stone-Fast and Simultaneous Analysis of Microplastics: Microparticles
493 Derived from Thermoplastics and Tire Wear. *Environ. Sci. Tech. Let.* **2018**, *5*, (10), 608-613.
- 494 20. Fischer, M.; Scholz-Bottcher, B. M., Simultaneous Trace Identification and
495 Quantification of Common Types of Microplastics in Environmental Samples by Pyrolysis-Gas
496 Chromatography-Mass Spectrometry. *Environ. Sci. Technol.* **2017**, *51*, (9), 5052-5060.
- 497 21. Fischer, M.; Scholz-Bottcher, B. M., Microplastics analysis in environmental samples -
498 recent pyrolysis-gas chromatography-mass spectrometry method improvements to increase the
499 reliability of mass-related data. *Anal Methods* **2019**, *11*, (18), 2489-2497.
- 500 22. Primpke, S.; Fischer, M.; Lorenz, C.; Gerdt, G.; Scholz-Bottcher, B. M., Comparison of
501 pyrolysis gas chromatography/mass spectrometry and hyperspectral FTIR imaging spectroscopy
502 for the analysis of microplastics. *Anal Bioanal Chem* **2020**, *412*, (30), 8283-8298.
- 503 23. Dumichen, E.; Eisentraut, P.; Celina, M.; Braun, U., Automated thermal extraction-
504 desorption gas chromatography mass spectrometry: A multifunctional tool for comprehensive
505 characterization of polymers and their degradation products. *Journal of Chromatography A*
506 **2019**, *1592*, 133-142.
- 507 24. Schirinzi, G. F.; Llorca, M.; Sero, R.; Moyano, E.; Barcelo, D.; Abad, E.; Farre, M.,
508 Trace analysis of polystyrene microplastics in natural waters. *Chemosphere* **2019**, *236*.
- 509 25. Sojak, L.; Kubinec, R.; Jurdakova, H.; Hajekova, E.; Bajus, M., High resolution gas
510 chromatographic-mass spectrometric analysis of polyethylene and polypropylene thermal
511 cracking products. *Journal of Analytical and Applied Pyrolysis* **2007**, *78*, (2), 387-399.
- 512 26. Dumichen, E.; Barthel, A. K.; Braun, U.; Bannick, C. G.; Brand, K.; Jekel, M.; Senz, R.,
513 Analysis of polyethylene microplastics in environmental samples, using a thermal decomposition
514 method. *Water Research* **2015**, *85*, 451-457.
- 515 27. Gomiero, A.; Oysaed, K. B.; Agustsson, T.; van Hoytema, N.; van Thiel, T.; Grati, F.,
516 First record of characterization, concentration and distribution of microplastics in coastal
517 sediments of an urban fjord in south west Norway using a thermal degradation method.
518 *Chemosphere* **2019**, *227*, 705-714.

- 519 28. Unice, K. M.; Kreider, M. L.; Panko, J. M., Use of a Deuterated Internal Standard with
520 Pyrolysis-GC/MS Dimeric Marker Analysis to Quantify Tire Tread Particles in the Environment.
521 *Int J Env Res Pub He* **2012**, *9*, (11), 4033-4055.
- 522 29. Dierkes, G.; Lauschke, T.; Becher, S.; Schumacher, H.; Foeldi, C.; Ternes, T.,
523 Quantification of microplastics in environmental samples via pressurized liquid extraction and
524 pyrolysis-gas chromatography. *Anal Bioanal Chem* **2019**, *411*, (26), 6959-6968.
- 525 30. Matsueda, M.; Mattonai, M.; Iwai, I.; Watanabe, A.; Teramae, N.; Robberson, W.;
526 Ohtani, H.; Kim, Y.-M.; Watanabe, C., Preparation and test of a reference mixture of eleven
527 polymers with deactivated inorganic diluent for microplastics analysis by pyrolysis-GC-MS.
528 *Journal of Analytical and Applied Pyrolysis* **2021**, *154*, 104993.
- 529 31. Hermabessiere, L.; Himber, C.; Boricaud, B.; Kazour, M.; Amara, R.; Cassone, A. L.;
530 Laurentie, M.; Paul-Pont, I.; Soudant, P.; Dehaut, A.; Duflos, G., Optimization, performance,
531 and application of a pyrolysis-GC/MS method for the identification of microplastics. *Anal*
532 *Bioanal Chem* **2018**, *410*, (25), 6663-6676.
- 533 32. Dumichen, E.; Eisentraut, P.; Bannick, C. G.; Barthel, A. K.; Senz, R.; Braun, U., Fast
534 identification of microplastics in complex environmental samples by a thermal degradation
535 method. *Chemosphere* **2017**, *174*, 572-584.
- 536 33. Tsuge, S.; Othani, H.; Watanabe, C., *Pyrolysis-GC/MS Data book of synthetic polymers*.
537 Elsevier: 2011.
- 538 34. Moldoneavu, C. C., *Analytical pyrolysis of synthetic organic polymers*. Elsevier ed.;
539 Elsevier: 2005.
- 540 35. Lauschke, T.; Dierkes, G.; Schweyen, P.; Ternes, T. A., Evaluation of poly(styrene-d5)
541 and poly(4-fluorostyrene) as internal standards for microplastics quantification by
542 thermoanalytical methods. *Journal of Analytical and Applied Pyrolysis* **2021**, *159*.
- 543 36. Bouzid, N.; Anquetil, C.; Dris, R.; Gasperi, J.; Tassin, B.; Derenne, S., Quantification of
544 Microplastics by Pyrolysis Coupled with Gas Chromatography and Mass Spectrometry in
545 Sediments: Challenges and Implications. *Microplastics* **2022**, *1*, (2), 229-239.
- 546 37. Ainali, N. M.; Bikiaris, D. N.; Lambropoulou, D. A., Aging effects on low- and high-
547 density polyethylene, polypropylene and polystyrene under UV irradiation: An insight into
548 decomposition mechanism by Py-GC/MS for microplastic analysis. *Journal of Analytical and*
549 *Applied Pyrolysis* **2021**, *158*.
- 550 38. Toapanta, T.; Okoffo, E. D.; Ede, S.; O'Brien, S.; Burrows, S. D.; Ribeiro, F.; Gallen, M.;
551 Colwell, J.; Whittaker, A. K.; Kaserzon, S.; Thomas, K. V., Influence of surface oxidation on the
552 quantification of polypropylene microplastics by pyrolysis gas chromatography mass
553 spectrometry. *Sci. Total Environ.* **2021**, *796*.
- 554 39. Mason, S. A.; Welch, V. G.; Neratko, J., Synthetic Polymer Contamination in Bottled
555 Water. *Frontiers in Chemistry* **2018**, *6*.
- 556 40. Ossmann, B. E.; Sarau, G.; Holtmannspotter, H.; Pischetsrieder, M.; Christiansen, S. H.;
557 Dicke, W., Small-sized microplastics and pigmented particles in bottled mineral water. *Water*
558 *Research* **2018**, *141*, 307-316.
- 559 41. Schymanski, D.; Goldbeck, C.; Humpf, H. U.; Furst, P., Analysis of microplastics in
560 water by micro-Raman spectroscopy: Release of plastic particles from different packaging into
561 mineral water. *Water Research* **2018**, *129*, 154-162.
- 562